

Received April 15, 2019, accepted May 19, 2019, date of publication May 29, 2019, date of current version June 11, 2019.

Digital Object Identifier 10.1109/ACCESS.2019.2919745

# Energy-Efficient Photoplethysmogram Compression to Estimate Heart and Respiratory Rates Simultaneously

**CHANKI PARK<sup>1</sup>, (Student Member, IEEE), AND BOREOM LEE<sup>2</sup>, (Member, IEEE)**

<sup>1</sup>School of Mechanical Engineering, Gwangju Institute of Science and Technology (GIST), Gwangju 61005, South Korea

<sup>2</sup>Department of Biomedical Science and Engineering (BMSE), Institute of Integrated Technology (IIT), Gwangju Institute of Science and Technology (GIST), Gwangju 61005, South Korea

Corresponding author: Boreom Lee (leebr@gist.ac.kr)

This work was supported in part by the Basic Science Research Program through the National Research Foundation of Korea (NRF) funded by the Ministry of Science and ICT under Grant 2017R1A2B4009068, and in part by the GIST Research Institute (GRI) Grant funded by the Gwangju Institute of Science and Technology (GIST), in 2019.

**ABSTRACT** A photoplethysmogram (PPG) sensor has been broadly used for smart watches and bands because it is easy to measure and contains many health information, such as heart rate (HR) and respiratory rate (RR). Because the PPG sensor blinks an LED at sampling instants, the rate for sampling and LED flashing should be reduced to extend the battery life. To reduce the rate, we employed two different compressive covariance sensing (CCS) techniques and applied them to HR and RR estimation. The CCS cannot recover a signal itself but reconstructs its covariance. We designed a signal processing technique to extract HR and RR from the reconstructed covariance. The estimation performance was evaluated by using the open-source data and the experimental data, and the power consumption of a wrist-type PPG sensor with respect to the compression ratio was evaluated. The proposed method acquired the covariance of the PPG with an average sampling rate of 1.79 Hz below the Nyquist rate for HR (10 Hz), and it significantly reduced the energy consumption for the PPG sampling. Moreover, its estimation accuracy was sufficient to be used for a wearable healthcare system. As a result, the proposed method showed that HR and RR can be estimated with an ultra-low-power PPG sensor.

**INDEX TERMS** Compressed sensing, health information and management, energy efficiency, photoplethysmogram.

## I. INTRODUCTION

Heart rate (HR) and respiratory rate (RR) are important information because they reflect various physical status. The change of HR is caused by sympathetic and parasympathetic nervous systems, the basic level of body metabolism, venous return determined by peripheral circulation, physical activity, age, and the size of the body. RR depends on chemical factor (blood oxygen level), nervous factor, and voluntary control [1]. According to the fast-growing usage of smart watches and smart bands with a photoplethysmogram (PPG) sensor, the technique to monitor users' HR and RR in daily life has attracted great attention [2]–[4]. HR can be estimated from the PPG by using frequency analysis techniques such as the Fourier transform, power spectral density, and an adaptive

The associate editor coordinating the review of this manuscript and approving it for publication was Sabah Mohammed.

notch filter. Because the respiratory component of the PPG is not clearly observed in the PPG, various signal processing techniques have been developed to estimate RR from the PPG.

There are three types of modulation of the PPG induced by respiration: amplitude, baseline, and pulse width modulations. Among these modulations, the baseline modulation can be understood as the presence of a frequency component; the frequency corresponds to RR. To extract the frequency component, digital filters were used [5]. For example, the respiratory component of PPG was acquired using a 0.6 Hz low-pass filter (LPF). An autoregressive (AR) model was frequently used for RR estimation [6], [7]. The poles of the AR model represent frequencies of the input signal and these are computed through a batch processing method. The concept was simple and the estimate was accurate. To implement a real-time operation, the AR model method

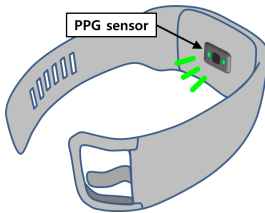


**FIGURE 1.** A smart band with a PPG sensor.

employed a moving-window technique yielding computational redundancy. In our previous study, we suggested an adaptive lattice-type respiratory rate estimator (ALRE) which utilizes an adaptive lattice notch filter (ALNF) as a frequency estimator [8]. The relation between designing a notch filter and finding AR model coefficients is theoretically similar and the ALRE can be interpreted as an adaptive version of the AR model method. As a result, it showed superior performance as well as has an efficient computational structure. Recently, the Holo-Hilbert spectral analysis based approach was proposed [9]. It can capture both frequency-modulated and amplitude-modulated features. However, it demands significant computational resources caused by an empirical mode decomposition (EMD). So far, many RR estimation algorithms have been developed using frequency analysis of PPG.

In spite of the development of smart watches, it is still important to extend battery life; the energy consumption of a PPG sensor determines the battery life. The PPG sensor illuminates the user's skin using a light-emitted diode (LED) and measures the change of blood volume by using the reflected light (see Fig. 1). Because the sensor should blink the LED at sampling instants to acquire a PPG, the rate for sampling and LED flashing is directly related to the energy consumption. A high rate will significantly reduce the battery life of smart watches or bands. To monitor the user's HR and RR for an extremely long time, an energy-efficient PPG sampling technique is required.

Compressed sensing (CS) is a representative technique that can analyze an original signal using a compressed signal sampled at a lower sampling rate than the Nyquist rate [10]. In previous studies, CS showed that electrophysiological signals (e.g., electromyogram and electrocardiogram) could be compressed with higher energy efficiency than wavelet-based compression techniques [11], [12]. Even though CS can compress a given analog signal through a measurement matrix, it cannot reduce the rate of LED pulses, for smart watches, because the light emission is essential to obtain the analog PPG [13].

As an alternative approach to CS, a new technique called compressive covariance sensing (CCS) has been proposed [14]. In the compression phase of CCS, the original signal is sampled with a specific pattern defined by a sparse ruler. Because no additional procedure is required for the compression (or sampling) phase of CCS, CCS can reduce

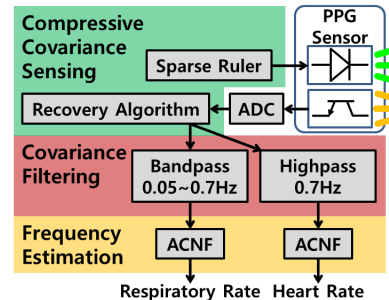


**FIGURE 2.** Block diagram representation of the proposed method.

the rate of sampling and LED flashing. Hence, we exploited the CCS to enhance the energy-efficiency of the PPG sensor. Daniel Romero and Greet Leus proposed the original CCS, which restores the covariance matrix of a non-sparse signal using a least square method [15]. We call it LS-CCS for convenience. Recently, we proposed an online CCS. Both the compression and recovery procedures of the online CCS are online processing [21]. It achieves a higher compression ratio than LS-CCS by using a circular sparse ruler (CSR). In this study, we considered only a covariance vector instead of the covariance matrix. Both CCS methods are described in section II in detail.

The CCS technique recovers the second-order statistics of an original signal from the compressed signal, but it cannot recover the original signal itself. Because covariance contains the frequency information of the original signal, CCS can be used to estimate HR and RR from a PPG. However, because the average sampling rate of CCS does not satisfy the Nyquist condition and the compressed signal is not equi-spaced data, conventional discrete-time signal processing techniques are unsuitable. Hence, we proposed an energy-efficient PPG sampling technique using CCS and designed new signal processing algorithms for CCS. The methods are explained in detail in the next section. In the results section, we compare the LS-CCS, online CCS, and ALRE using open-source data and wrist-type PPG signals. In the discussion section, the experimental results are interpreted and discussed.

## II. METHODS

The proposed PPG sampling technique consists of three steps as shown in Fig. 2. In the first step, the PPG makes the LED blink with the pattern of a sparse ruler, and then measures the reflected light; the sparse ruler determines the rate of LED pulses. From the measured samples (see Fig. 3), it reconstructs a covariance of PPG using a recovery algorithm. These processes correspond to the compression and recovery phases of CCS. We adopted two different CCSs (LS-CCS or online CCS) and these are explained in the next subsections. In the second step, cardiac and respiratory components are extracted from the reconstructed covariance, and then HR and RR are estimated using a frequency estimator.

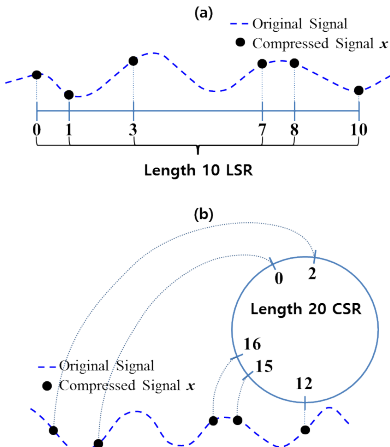


**FIGURE 3.** Sampling pattern and sparse rulers. (a) A length-10 LSR. (b) A length-20 CSR.

For computational efficiency, we designed an adaptive covariance notch filter (ACNF) to estimate the frequencies (HR and RR).

#### A. COMPRESSIVE COVARIANCE SENSING

CCS consists of a compression phase and a recovery phase. In the compression phase, CCS employs a sparse ruler as a sampling pattern. There are two kinds of sparse rulers (see Fig. 3): a linear sparse ruler (LSR) and a circular sparse ruler (CSR). A length- $(N - 1)$  sparse ruler has  $M$  marks, which are integers between 0 and  $N - 1$  ( $M \ll N$ ), and a set of the marks is  $S \subset \{0, \dots, N - 1\}$ .  $S$  is a length- $(N - 1)$  LSR when there exists at least one pair of elements  $s$  and  $s'$  in  $S$  for all integers  $l$  between 0 and  $N - 1$  such that

$$s - s' = l \quad (1)$$

where  $s \geq s'$ . In the same manner,  $S$  is a length- $(N - 1)$  CSR, if for any integer  $l$  from 0 to  $N - 1$  there is one or more pairs  $s$  and  $s'$  in  $S$  such that

$$(s - s') \% N = l \quad (2)$$

where  $\%$  is a modulo operator. The compression ratio is  $M/N$ . When a sparse ruler  $S$  has the least number of marks, then  $S$  has an optimal compression ratio and is called a minimal sparse ruler. By the concatenation of the same  $B$  sparse rulers, a length- $(L - 1)$  sparse ruler is implemented ( $L = B \times N$ ), and the number of marks  $K$  is  $B \times M$ . The  $L$  will be the length of the estimated covariance.

The compression phase is an underdetermined system, but it can be transformed into an overdetermined system by assuming that the covariance matrix has a specific structure such as Toeplitz and circulant. The original CCS solves the transformed overdetermined model using a least-square method; we call it LS-CCS. The original LS-CCS employed an LSR in the compression phase. The full procedure of LS-CCS is described in [14] in detail.

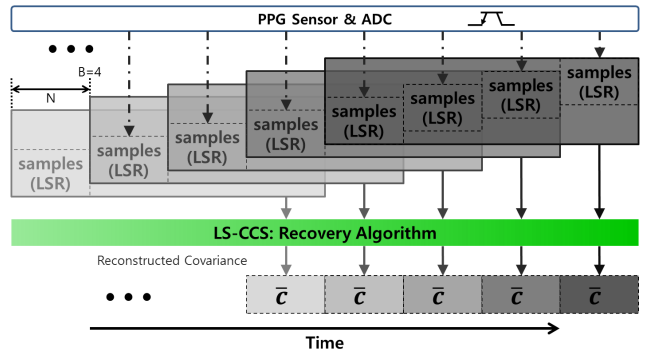


**FIGURE 4.** Real-time implementation of LS-CCS.

The LS-CCS assumes the original signal is wide-sense stationarity (WSS) and the estimated covariance is calculated over a length- $(L - 1)$  LSR; its temporal resolution is insufficient. To implement real-time estimation, we employ a moving window technique as shown in Fig 4. The length  $L$  covariance is calculated from recent  $B$  LSRs, and the estimate is updated at the end of each LSR. Because there is an overlap of  $(B - 1) \times N$  samples at each time window, this real-time implementation has computational redundancy.

#### B. ONLINE COMPRESSIVE COVARIANCE SENSING

In our previous study, we proposed an online CCS [21]. It has several advantages over the LS-CCS. First, it utilized a CSR having a higher compressibility than a length  $(N - 1)$  LSR, generally [16]. Second, its temporal resolution is better than that of LS-CCS, because the online CCS updates the estimate at every mark. Last, because the recovery algorithm of the online CCS is operated by a recursive formulation, there is no computational redundancy, unlike the real-time implementation of LSR.

In the compression phase, the online CCS samples the signal with the pattern of a CSR (see Fig. 3). Pairs of the new sample values and the corresponding mark indices are stored in a two-dimensional queue  $D = [\mathbf{x}, \mathbf{i}]$ .  $\mathbf{x}$  consists of sample values and  $\mathbf{i}$  represents their marks. After sampling and enqueueing, the covariance recovery algorithm is immediately operated using the updated queue  $D$ . The recovery algorithm is described in Algorithm 1.

#### C. COVARIANCE FILTERING

Because the feasible ranges of RR are HR are different, a digital filtering technique can extract cardiac and respiratory components. However, most discrete-time signal processing techniques are not applicable to CCS, because not only does the CCS not satisfy the Nyquist condition but also the samples are not uniformly spaced. To solve this problem, we exploit the relation between the covariance of the filtered signal  $\mathbf{y}$  and input signal  $\mathbf{x}$  [17] as follows:

$$\mathbf{y}[n] = h[n] * \mathbf{x}[n] \quad (3)$$

$$c_y[l] = c_x[l] * h[l] * h^*[-l] \quad (4)$$

**Algorithm 1** Covariance Recovery of Online CCS

---

**Input:** samples at iteration  $m \mathbf{x} = [x(1), \dots, x(K)]^T$ ,  
sample marks  $\mathbf{i} = [i(1), \dots, i(K)]^T$ ,  
and recovered covariance sequence at iteration  $m - 1$   
 $\bar{\mathbf{c}}(m-1) = [\bar{c}(0, m-1), \dots, \bar{c}(L-1, m-1)]^T$

**Output:** recovered covariance sequence at iteration  $m$   
 $\bar{\mathbf{c}}(m) = [\bar{c}(0, m), \dots, \bar{c}(L-1, m)]^T$

---

$\bar{\mathbf{c}}(m) = \bar{\mathbf{c}}(m-1)$   
**for**  $j = 0 : B - 1$   
    **for**  $k = 1 : M$   
         $l = (i(k + Mj) - i(1)) \%N + Nj$   
         $\bar{c}(l, m) = \lambda \bar{c}(l, m) + (1 - \lambda)x(1) \cdot x^*(k + Mj)$   
    **end**  
**end**  
\* %: modulo operator

---

where  $h[n]$  represents the impulse response of the digital filter.  $c_y$  and  $c_x$  are the covariances of the filtered signal  $y$  and the input signal  $x$ . As shown in (4), the covariance of the filtered signal can be calculated by forward-backward filtering of the reconstructed covariance [18]. In this study, a Butterworth filter was employed to enhance the HR and RR. A 0.7 Hz high pass filter and a 0.05–0.7 Hz bandpass filter were used for HR and RR estimation, respectively.

**D. FREQUENCY ESTIMATION**

Because the covariance contains the frequency information of the original signal, the HR and RR can be estimated by using a Fourier transform; the Fourier transform of covariance is the power spectral density. Maximum values of the spectrum will correspond to HR and RR, but it is inefficient to operate these processes at each iteration. Hence, we designed an adaptive covariance notch filter (ACNF) which serves as a frequency estimator. The ACNF is based on a 2<sup>nd</sup> order infinite impulse response (IIR) notch filter as follows:

$$H(z) = \frac{1 - 2az^{-1} + z^{-2}}{1 - (1+r)az^{-1} + rz^{-2}} \quad (5)$$

$$a = \cos(\omega_0) \quad (6)$$

where  $\omega_0$  represents notch frequency.  $a$  and  $r$  are the coefficients of the all-zero filter, and the pole-and-zero contraction factor ( $0 \leq r < 1$ ), respectively. The notch filter (5) can be expressed as difference equations as follows:

$$s[l] = c_y[l] + (1+r)as[l-1] - rs[l-2] \quad (7-1)$$

$$e[l] = s[l] - 2as[l-1] + s[l-2] \quad (7-2)$$

where  $s[l]$  is the output of the all-pole filter, and  $e[l]$  is the output of the notch filter. We set the cost function as follows:

$$J[l] \equiv E[e^2[l]] \quad (8)$$

where  $E[\cdot]$  means ensemble average. By optimization of the cost function  $J[l]$  with respect to  $a$ , we can find the optimal  $a$  as follows:

$$\frac{\partial J[l]}{\partial a} = E[-2e[l]s[l-1]] = 0 \quad (9)$$

$$a[l] = \frac{E[\{s[l] + s[l-2]\}s[l-1]]}{2E[s^2[l-1]]} \quad (10)$$

To compute  $a[l]$ , we replace the ensemble average with a sample mean. The estimated frequency is calculated as follows:

$$\hat{\omega}_0[l] = \cos^{-1}(a[l]) \quad (11)$$

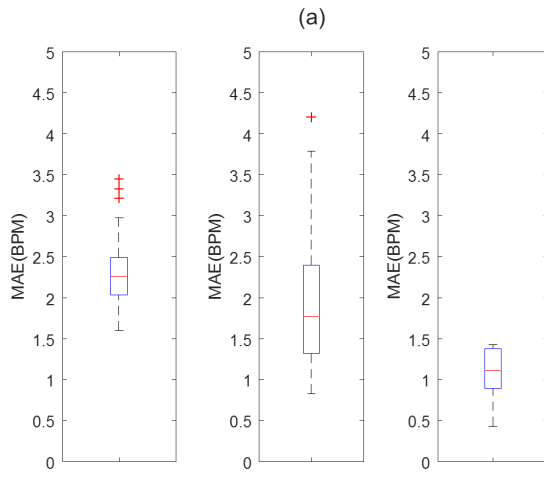
The input of the ACNF is the filtered covariance and its estimate corresponds to HR or RR (see Fig. 2). The ACNF can be interpreted as the batch version of ALNF [19].

**E. DATA COLLECTION**

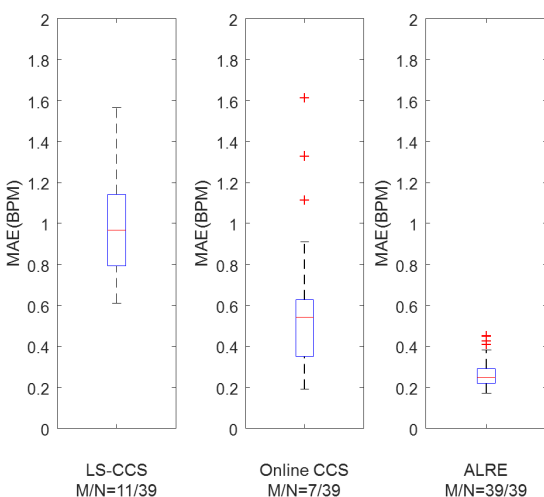
We used an MIT MIMIC Database and isolated 50 data sets which were less contaminated by artifacts [20]. Each data set was recorded at a sampling rate of 125 Hz for 9 min 40 s. It included the PPG, ECG, and respiratory signal. Because the feasible range of HR is 0.5–5 Hz, we down-sampled the signals to 10.4167 Hz. Additionally, we collected wrist-type PPG, ECG, and respiratory signals from four male and one female subjects (Age = 27 ± 2.6 years). All subjects were instructed to take a breath randomly and participated in six trials. In total, 30 data sets were collected. We utilized a SON1303 sensor as the wrist-type PPG sensor and the signal was sampled by an Atmel ATmega 328 with a sampling rate of 10 Hz. To implement energy-efficient sampling, we adjusted the intensity of the LED of the sensor as low as possible and set it to blink with a pulse width of 25 ms. The ECG and respiratory signal were measured by a BIOPAC® and its sampling frequency was 1000 Hz. All signals were recorded for 5 min and were synchronized. The peaks of the ECG were used to acquire the reference HR, and the reference RR was calculated from the zero crossing values of the respiratory signal. To evaluate energy consumption, we connected a 10.1 Ω resistor between a power source and the wrist-type PPG system and acquired the current by measuring the voltage across the resistor [11]. The LED flashing and sampling pattern, with a sparse ruler, were implemented on the Atmel ATmega328. The institutional review board of the Gwangju Institute of Science and Technology approved all procedures in this study.

**III. RESULTS**

We proposed an energy-efficient HR and RR estimation method using CCS and evaluated each result for two different types of CCS (LS-CCS and online CCS). The HR and RR estimation performance of the proposed method was compared with that of ALRE. Because there is no compression for ALRE, the compression ratio ( $M/N$ ) of ALRE is 1. We used a length-38 LSR ( $M/N = 11/39$ ) for LS-CCS and a length-38 CSR ( $M/N = 7/39$ ) for the online CCS. Both sparse rulers are minimal sparse rulers. To obtain sufficient covariance length, we set  $B = 5$ . Because convergence time is required for the frequency estimation, we excluded the initial 25 sec from our analysis. The performance of the method was evaluated through the mean absolute error (MAE) between estimated RR and reference RR, and between the estimated



(a)

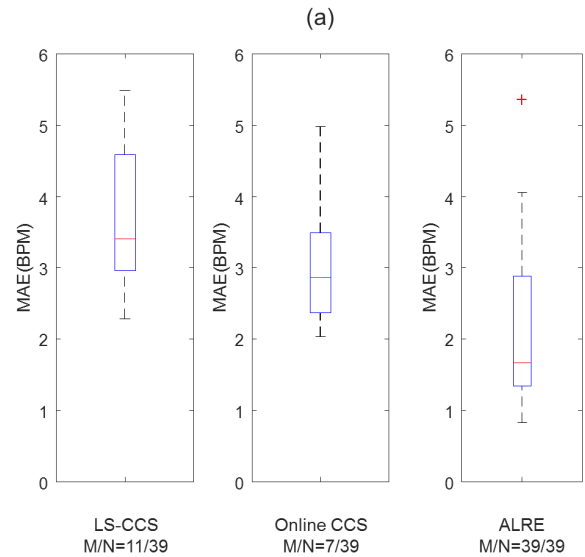


(b)

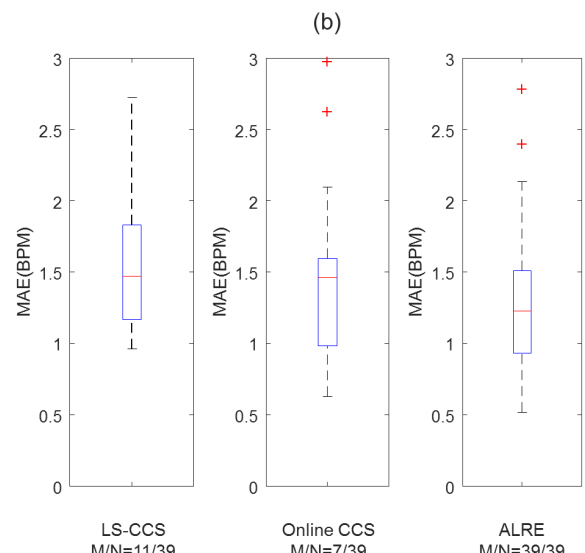
**FIGURE 5.** Distribution of MAE of HR and RR estimation for MIT MIMIC open source data. HR and RR are estimated by each method (LS-CCS, Online CCS, and ALRE). Upper and lower boxes represent the distribution of MAEs from 25th to 75th percentiles. Top and bottom lines indicate the 90th and 10th percentiles. (a) and (b) depict the results for HR and RR, respectively.

HR and reference HR. For a fair comparison, we adopted the parameters of each method, which minimized the MAE.

First, we evaluated the HR and RR estimation performance using the Massachusetts Institute of Technology (MIT) multiparameter intelligent monitoring in intensive care (MIMIC) data. As shown in Fig. 5, the HR and RR estimates of the ALRE ( $M/N = 1$ ) showed best estimation accuracy; however, its compression ratio  $M/N = 1$ . Although the proposed approach does not have better performance than ALRE, the compression ratio of LS-CCS is  $M/N = 11/39$  and that of online CCS is  $7/39$ . It was shown that the online CCS leads to better estimation performance than the LS-CCS. We performed statistical tests by using a paired t-test between the estimate of online CCS and that of other methods (the LS-CCS based method and ALRE). There was a significant



(a)



(b)

**FIGURE 6.** Distribution of MAE of HR and RR estimation for our experimental data. HR and RR are estimated by each method (LS-CCS, Online CCS, and ALRE). Upper and lower boxes represent the distribution of MAEs from 25th to 75th percentiles. Top and bottom lines indicate the 90th and 10th percentiles. (a) and (b) depict the results for HR and RR, respectively.

difference between the HR estimate of online CCS and that of LS-CCS ( $p < 0.05$ ), and there was an extremely significant difference between the HR estimate of online CCS and that of ALRE ( $p < 0.005$ ). In the case of RR estimation, all p-values were less than 0.005 for all comparisons (online CCS vs. LS-CCS and ALRE vs. online CCS). In our experimental data, the estimation performance of all methods shows the similar tendency as the result for the MIT MIMIC data (see Fig. 6). We performed statistical tests on our experimental data with the non-parametric Wilcoxon's two-sample signed-rank test between the estimate of online CCS and that of other methods. In the case of HR estimation, all p-values were less than 0.005 for all comparisons (online CCS vs. LS-CCS and ALRE vs. online CCS). There was an extremely significant

**TABLE 1.** The energy consumption necessary for flashing an led and sampling an analog Ppg.

Compression Ratio ( $M/N$ )	7/39	11/39	39/39
Energy Consumption (mW)	1.8	2.0	3.1

difference between the RR estimate of online CCS and that of ALRE ( $p < 0.005$ ), but there was no significant difference between the RR estimate of online CCS and that of LS-CCS.

We evaluated the energy consumption of each method for LED flashing and sampling. The average sampling rates of ALRE, LS-CCS, and online CCS were 10 Hz, 2.82 Hz, and 1.79 Hz, respectively. Table 1 shows the energy consumption for flashing an LED and sampling an analog PPG. A compression ratio of 39/39 denotes no compression.

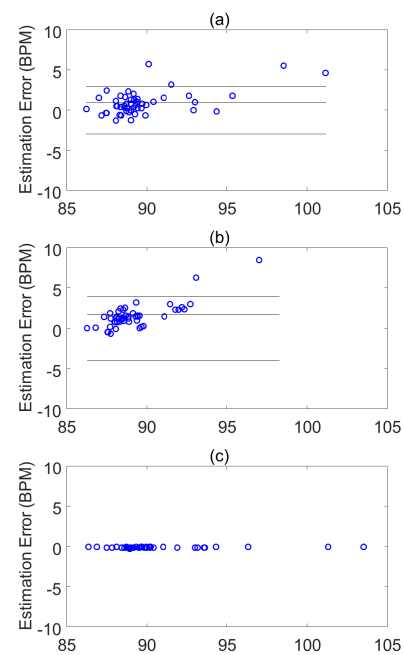
#### IV. DISCUSSION

HR and RR are the most crucial items of health information. It is difficult to estimate RR from a PPG because the respiratory component is not clearly observed in the PPG. Advanced signal processing techniques, such as digital filters [5], AR models [6], and adaptive filters [8], have been used to estimate RR. We proposed an energy-efficient PPG covariance sampling technique using CCS and designed an algorithm to estimate the HR and RR from the reconstructed covariance of PPG.

Because PPG is obtained by measuring the reflected light from the skin, the LED should flash at the timing for sampling. It is very important to reduce the rate for LED flashing and sampling to enhance the energy-efficiency of a PPG sensor. Conventional CS cannot reduce the number of LED flashes, but CCS can reduce the rate.

Daniel Romero and Greet Leus first proposed CCS using a least square method [15]. LS-CCS is an innovative sampling technique, but LS-CCS has several limitations. First, the temporal resolution is not good, because it is a batch process. Second, its huge dimensionality can lead an insufficient memory condition. Last, it was designed using an LSR. A CSR, generally, has a better compression ratio than an LSR. In order to compensate for the temporal resolution of LS-CCS, we designed a scheme for real-time implementation (see Fig. 4). The recently proposed online CCS not only compresses the signal through a CSR but also performs the covariance recovery with online processing [21]. Therefore, the online CCS has better compression and temporal resolution than LS-CCS. Although the real-time implementation scheme for LS-CCS causes computational redundancy, the online CCS does not have such redundancy and has lower computational complexity than LS-CCS.

Because the signal obtained by CCS is not equi-spaced data, conventional signal processing techniques cannot be applied; therefore, covariance filtering is proposed instead of digital filtering. Covariance filtering can be implemented by forward-backward filtering [18]. Although HR and RR can be estimated by analyzing the frequency of the reconstructed covariance, frequency analysis such as using the

**FIGURE 7.** Bland Altman plot for HR estimation (MIT-MIMIC data). (a) Online CCS; (b) LS-CCS; (c) ALRE.

Fourier transform is inefficient to trace HR and RR. The proposed ACNF can recursively track HR and RR with a light computation load. The ACNF can be interpreted as a batch version of ALNF [19].

Generally, the compressibility of compression methods (e.g., wavelet transform and compressed sensing) is inversely proportional to their performance. In the case of CCS, the number of marks of a sparse ruler determines the compression ratio of CCS. In this study, we used a minimal sparse ruler, which has the least number of marks. Even though the number of marks increases, all elements of the covariance are not uniformly restored, but only some elements are repeatedly reconstructed. Hence, there was no significant difference in estimation performance between sparse rulers with the same length and different compression ratios.

Unlike conventional compression techniques, CCS compresses a signal according to a sparse ruler without any criterion. This feature can implement an energy-efficient PPG compression system but results in loss of informative data and poor estimation accuracy. Hence, the estimate of CCS was shown to be less accurate than that of ALRE (see Fig. 7). Even though the estimation performance of online CCS is lower than that of ALRE, most of the estimation errors were less than 5% and it is sufficiently useful in healthcare applications [21]. We expect that advanced signal processing techniques will enhance the estimation accuracy of online CCS.

HR and RR estimation performance was evaluated using the MIT-MIMIC open source database and our experimental data. The estimation accuracy of ALRE was the best. The online CCS not only has better compression ratio than the LS-CCS but also showed good HR and RR estimation

performance. The online CCS showed the highest efficiency in terms of energy consumption (see Table 1). The online CCS acquires the covariance of PPG with an average sampling rate of 1.79 Hz, below Nyquist rate for HR (10 Hz).

## V. CONCLUSION

We proposed an energy-efficient PPG compression technique and applied it to HR and RR estimation. The HR and RR estimation method based on the online CCS reduced the sampling and LED flash rate by 1.79 Hz and showed a high estimation accuracy. We expect that this energy-efficient PPG compression technique will be widely used for a smart watch and band. In future work, we will develop an advanced signal processing technique to enhance the estimation accuracy of the CCS technique.

## REFERENCES

- [1] A. Guyton and J. Hall, *Textbook of Medical Physiology*, 9th ed. Philadelphia, PA, USA: Elsevier Saunders, 1996.
- [2] T. Tamura, Y. Maeda, M. Sekine, and M. Yoshida, "Wearable photoplethysmographic sensors—Past and present," *Electronics*, vol. 3, no. 2, pp. 282–302, Apr. 2014.
- [3] Z. Zhang, Z. Pi, and B. Liu, "TROIKA: A general framework for heart rate monitoring using wrist-type photoplethysmographic signals during intensive physical exercise," *IEEE Trans. Biomed. Eng.*, vol. 62, no. 2, pp. 522–531, Feb. 2015.
- [4] P. Renevey, R. Delgado-Gonzalo, A. Lemkadem, C. Verjus, S. Combertaldi, B. Rasch, B. Leeners, F. Dammeier, and F. Kübler, "Respiratory and cardiac monitoring at night using a wrist wearable optical system," in *Proc. IEEE 40th Annu. Int. Conf. Eng. Med. Biol. Soc. (EMBC)*, Jul. 2018, pp. 2861–2864.
- [5] K. Nakajima, T. Tamura, and H. Miike, "Monitoring of heart and respiratory rates by photoplethysmography using a digital filtering technique," *Med. Eng. Phys.*, vol. 18, pp. 365–372, Jul. 1996.
- [6] S. G. Fleming and L. Tarassenko, "A comparison of signal processing techniques for the extraction of breathing rate from the photoplethysmogram," *Int. J. Biol. Med. Sci.*, vol. 2, no. 4, pp. 232–236, 2007.
- [7] J. Lee and K. H. Chon, "Respiratory rate extraction via an autoregressive model using the optimal parameter search criterion," *Ann. Biomed. Eng.*, vol. 38, no. 10, pp. 3218–3225, Oct. 2010.
- [8] C. Park and B. Lee, "Real-time estimation of respiratory rate from a photoplethysmogram using an adaptive lattice notch filter," *Biomed. Eng. Online*, vol. 13, no. 1, p. 170, Jan. 2014.
- [9] H.-H. Chang, C.-C. Hsu, C.-Y. Chen, W.-K. Lee, H.-T. Hsu, K.-K. Shyu, J.-R. Yeh, P.-J. Lin, and P.-L. Lee, "A method for respiration rate detection in wrist PPG signal using Holo-Hilbert spectrum," *IEEE Sensors J.*, vol. 18, no. 18, pp. 7560–7569, Sep. 2018.
- [10] D. L. Donoho, "Compressed sensing," *IEEE Trans. Inf. Theory*, vol. 52, no. 4, pp. 1289–1306, Apr. 2006.
- [11] H. Mamaghanian, N. Khaled, D. Atienza, and P. Vandergheynst, "Compressed sensing for real-time energy-efficient ECG compression on wireless body sensor nodes," *IEEE Trans. Biomed. Eng.*, vol. 58, no. 9, pp. 2456–2466, Sep. 2011.
- [12] A. M. R. Dixon, E. G. Allstot, D. Gangopadhyay, and D. J. Allstot, "Compressed sensing system considerations for ECG and EMG wireless biosensors," *IEEE Trans. Biomed. Circuits Syst.*, vol. 6, no. 2, pp. 156–166, Apr. 2012.
- [13] D. Craven, B. McGinley, L. Kilmartin, M. Glavin, and E. Jones, "Compressed sensing for bioelectric signals: A review," *IEEE J. Biomed. Health Inform.*, vol. 19, no. 2, pp. 529–540, Mar. 2015.
- [14] D. Romero, D. D. Ariananda, Z. Tian, and G. Leus, "Compressive covariance sensing: Structure-based compressive sensing beyond sparsity," *IEEE Signal Process. Mag.*, vol. 33, no. 1, pp. 78–93, Jan. 2016.
- [15] D. Romero and G. Leus, "Compressive covariance sampling," in *Proc. Inf. Theory Appl. Workshop (ITA)*, Feb. 2013, pp. 1–8.
- [16] D. Romero, R. López-Valcarce, and G. Leus, "Compression limits for random vectors with linearly parameterized second-order statistics," *IEEE Trans. Inf. Theory*, vol. 61, no. 3, pp. 1410–1425, Mar. 2015.
- [17] M. H. Hayes, *Statistical Digital Signal Processing and Modeling*. New York, NY, USA: Wiley, 1996.
- [18] C. Park, H. Shin, and B. Lee, "Blockwise PPG enhancement based on time-variant zero-phase harmonic notch filtering," *Sensors*, vol. 17, no. 4, p. 860, 2017.
- [19] N. I. Cho and S. U. Lee, "On the adaptive lattice notch filter for the detection of sinusoids," *IEEE Trans. Circuits Syst. II, Analog Digit. Signal Process.*, vol. 40, no. 7, pp. 405–416, Jul. 1993.
- [20] A. L. Goldberger, L. A. N. Amaral, L. Glass, J. M. Hausdorff, P. C. Ivanov, R. G. Mark, J. E. Mietus, G. B. Moody, C.-K. Peng, and H. E. Stanley, "PhysioBank, PhysioToolkit, and PhysioNet: Components of a new research resource for complex physiologic signals," *Circulation*, vol. 101, no. 23, pp. e215–e220, Jun. 2000.
- [21] A. Shcherbina, C. M. Mattsson, D. Waggett, H. Salisbury, J. W. Christle, T. Hastie, M. T. Wheeler, and E. A. Ashley, "Accuracy in wrist-worn, sensor-based measurements of heart rate and energy expenditure in a diverse cohort," *J. Pers. Med.*, vol. 7, no. 2, p. 3, May 2017.



**CHANKI PARK** received the B.S. degree in control and instrumentation engineering from the Seoul National University of Science and Technology, Seoul, South Korea, in 2011, and the M.S. degree from the School of Mechatronics, Gwangju Institute of Science and Technology (GIST), Gwangju, South Korea, in 2014, where he is currently pursuing the Ph.D. degree with the School of Mechanical Engineering. His current research interests include compressive sensing and biomedical signal processing.



**BOREOM LEE** graduated from the Seoul National University College of Medicine, Seoul, South Korea. He received the M.D. degree, in 1998 and the Ph.D. degree in biomedical engineering from Seoul National University, in 2007. He joined the faculty of the Gwangju Institute of Science and Technology (GIST), in 2011, where he is currently an Associate Professor with the Department of Biomedical Science and Engineering (BMSE). His current research interests include brain connectomics, healthcare systems, biomedical signal processing and instrumentation, and machine learning application in medical research areas.